Article

J. Mex. Chem. Soc. **2025**, *69*(3)
Regular Issue

ISSN-e 2594-0317

Chemical Upcycling of Waste Polyethylene Terephthalate *via* Cosolvent-Assisted Alkaline Hydrolysis

---

Gaurav Kumar, Anand Bharti*

Department of Chemical Engineering, Birla Institute of Technology Mesra, Ranchi, Jharkhand, India – 835215.

***Corresponding author:** Anand Bharti, e-mail: abharti@bitmesra.ac.in

Received January 27th, 2024; Accepted September 3rd, 2024.

DOI: http://dx.doi.org/10.29356/jmcs.v69i3.2206

Abstract. Alkaline hydrolysis is a chemical recycling process for depolymerizing waste polyethylene terephthalate (PET) into monomers. These monomers can be used as a starting material to produce PET with the same quality as the original polymer. But conventional alkaline hydrolysis is carried out at a high temperature for a long reaction time which increases the capital and operating cost of the overall process. Therefore, developing an efficient method for PET depolymerization under mild reaction conditions is necessary to make upcycling an economically attractive process. In this work, the alkaline hydrolysis of waste PET was carried out with *n*-propanol as a co-solvent under mild conditions (70 °C). Sodium hydroxide (NaOH) was used as a catalyst. The effects of process parameters such as reaction time (15-60 min), co-solvent volume ratio (20 %, 40 %, and 60 %), and NaOH concentration (5 % and 15 % wt/vol) were examined on PET conversion and monomer (terephthalic acid (TPA)) yield. At optimal conditions (60:40 vol% *n*-propanol: H_2O, 15 wt% NaOH, 70 °C, 45 minutes), %PET conversion and %TPA yield obtained was 91.4 % and 71.3 %, respectively. Differential scanning calorimetry (DSC), powder X-ray diffraction (p-XRD), thermogravimetric analysis (TGA), nuclear magnetic resonance spectroscopy (NMR) and Fourier-transform infrared spectroscopy (FTIR) were used to assess the purity of the produced TPA. PET depolymerization kinetics was studied with the help of solid-state kinetic models. The best-fit kinetic models were a first-order reaction, geometrical contraction, and one-dimensional diffusion models. The energy economy coefficient, energy metrics, was used to compare the performance of *n*-propanol as a co-solvent with other co-solvents reported in the literature. It was found that *n*-propanol as a co-solvent is as efficient as ethanol at high NaOH concentration (15 wt/vol%).
Keywords: PET; chemical upcycling; alkaline hydrolysis; TPA; energy economy coefficient.

Resumen. La hidrólisis alcalina es un proceso de reciclaje químico utilizado para despolimerizar residuos de polietilentereftalato (PET) en monómeros. Estos monómeros pueden emplearse como materia prima para producir PET con la misma calidad que el polímero original. Sin embargo, la hidrólisis alcalina convencional se lleva a cabo a alta temperatura y durante un tiempo prolongado de reacción, lo que incrementa los costos de inversión y operación del proceso. Por ello, es necesario desarrollar un método eficiente para la despolimerización del PET bajo condiciones suaves de reacción, a fin de que el reciclaje ascendente sea un proceso económicamente atractivo. En este trabajo, la hidrólisis alcalina de residuos de PET se realizó utilizando n-propanol como cosolvente bajo condiciones suaves (70 °C). Se utilizó hidróxido de sodio (NaOH) como catalizador. Se estudiaron los efectos de parámetros del proceso como el tiempo de reacción (15-60 minutos), la proporción de volumen del cosolvente (20 %, 40 % y 60 %) y la concentración de NaOH (5 % y 15 % peso/volumen) sobre la conversión del PET y el rendimiento de monómero (ácido tereftálico, TPA). En las condiciones óptimas (60:40 % vol n-propanol:agua, 15 % peso/vol NaOH, 70 °C, 45 minutos), se obtuvo un 91.4 % de conversión de PET y un 71.3 % de rendimiento de TPA. Se utilizaron calorimetría diferencial de barrido (DSC), difracción de rayos X en polvo (p-XRD), análisis termogravimétrico (TGA), espectroscopía de resonancia magnética nuclear (RMN) y espectroscopía infrarroja por transformada de Fourier (FTIR) para

ISSN-e 2594-0317

evaluar la pureza del TPA producido. La cinética de despolimerización del PET se estudió con la ayuda de modelos cinéticos en estado sólido. Los modelos cinéticos que mejor se ajustaron fueron el de reacción de primer orden, contracción geométrica y difusión unidimensional. El coeficiente de economía energética, o métricas energéticas, se utilizó para comparar el desempeño del n-propanol como cosolvente con otros cosolventes reportados en la literatura. Se encontró que el n-propanol como cosolvente es tan eficiente como el etanol a una alta concentración de NaOH (15 % peso/vol).
Palabras clave: PET; reciclaje químico ascendente; hidrólisis alcalina; TPA; coeficiente de economía energética.

Introduction

Polyethylene terephthalate (PET) is a type of thermoplastic polymer resin and one of the world's most versatile and widely used plastics. It is highly resistant to impact, chemical degradation, and temperature changes, making it ideal for use in various products. PET has good gas and moisture barrier properties and is also low in weight, which makes it an excellent material for packaging and transportation. Plastic is also used for textile fibers, industrial and engineering purposes, and medical implants. The production of PET has increased from 6.6 MMT in 1990 to 74 MMT in 2021[1,2].

But due to inefficient waste plastic management, most of these plastics, after use, are not recycled and therefore accumulate in landfills. Only 9 % of the nearly 6300 MMT of plastic garbage produced between 1950 and 2015 was recycled, 12 % burned, and the remaining 79 % ended up in landfills [3]. As per the most recent data, 16 % of waste plastics have been recycled, 25 % have been incinerated, 40% have accumulated in landfills, and 19 % have ended up in unmanaged dumps [4]. An estimated 4.8 to 12.7 MMT of plastic waste enters the ocean yearly [5]. These plastics remain in the sea for years, either in their original form or as small particles. Recycling could solve the issue caused by the generation of waste plastic. PET recycling can be categorized into four major methods: primary, secondary, tertiary, and quaternary. Primary recycling, also known as re-extrusion, directly recycles off-spec grade pre-consumer PET into the production process. This process uses clean and uncontaminated PET as the feedstock and makes the process economical. Secondary recycling, often called mechanical recycling, is the process of recycling post-consumer PET through physical reprocessing. It is the most widely adopted process for large-scale recycling of post-consumer PET waste. Tertiary recycling, also known as chemical recycling, is the process in which PET is depolymerized into monomers, dimers, oligomers, and other chemicals. After purification, these products can be used to produce the original material or as feedstock for various valuable products. Chemical recycling is carried out either by solvolysis or pyrolysis. Solvolysis is a chemical recycling process in which the depolymerization of PET is carried out in the presence of a solvent. In contrast, pyrolysis occurs without oxygen or air or in a vacuum. Quaternary recycling is incinerating PET waste, and some energy is recovered from heat. The polymer is lost, releasing hazardous gases and leaving toxic residues behind [6–14].

Most post-consumer PET is recycled through mechanical recycling. The disadvantage of this process is that the hydrolysis and transesterification reactions in the polymer chains cause the product's quality to deteriorate in each cycle, eventually leading to lower-value materials [15,16]. It is believed that chemical recycling of PET waste will make the cycle circular and lead toward sustainable development.

Chemical recycling processes are typically divided into five categories, depending on the type of solvent employed, hydrolysis, alcoholysis, glycolysis, aminolysis, and ammonolysis. The development of the hydrolysis process, which involves the depolymerization of PET using water as a solvent, is the subject of growing research. It can be carried out under three conditions: neutral, alkaline, or acidic. The reaction is usually carried out at a high temperature and pressure with prolonged reaction time, and terephthalic acid (TPA) and ethylene glycol (EG) are the major products. Few works are reported in the literature on the hydrolysis of PET. Lian-Chun Hu et al. investigated the alkali-based depolymerization of PET with methanol or ethanol as a solvent. Ethers such as dioxane, tetrahydrofuran, or 1,2-dimethoxyethane were added as a co-solvent to study the effect on decomposition rate. It was observed that the addition of ethers accelerated the rate of PET decomposition, and the optimum result was obtained with dioxane (10 vol%) in methanol at 60 °C in 40 min [17]. V. A. Kosmidis et al. studied phase transfer catalyzed alkali decomposition of PET.

Trioctylmethylammonium bromide (TOMAB) was used as a phase transfer catalyst and was observed to be efficient for preparing pure TPA. Without a catalyst for a reaction time of 5 h, the TPA yield was 7 %, whereas the yield was 90 % with 0.01 mol TOMAB/mol PET [18]. G. P. Karayannidis et al. studied PET depolymerization in a stainless-steel autoclave with the help of an aqueous NaOH solution (1.125 M). A TPA yield of 97.9 % was obtained at 200 °C in 60 min [19]. Mishra et al. studied PET waste's alkaline hydrolysis using sodium hydroxide, keeping the PH at 14 by adding piperidine. It was concluded that the ratio of 10:7 of PET waste: sodium hydroxide for 2.5 h gave 85 % of TPA as the optimum yield [20]. In another work, Mishra et al. studied the depolymerization of PET in an aqueous NaOH solution by varying the temperature and time. Under optimum conditions (Temp = 150 °C, Time = 90 min, charge ratios (moles of NaOH/ moles of PET repeating units charged = 4), 98.52 % PET conversion and 98.46 % TPA yield were obtained [21]. PET hydrolysis was carried out in an alkaline environment by H. I. Khalaf et al. utilizing a microwave reactor and quaternary ammonium salt as a phase transition catalyst. Under optimum conditions (200 W power and 3 % wt./wt. PTC/PET), 99 % of TPA was obtained with 10 % NaOH in 60 min [22]. Ugduler et al. conducted an interesting study on waste PET degradation at atmospheric pressure and mild temperature conditions. The effect of various parameters such as temperature (50-80 °C), ethanol: water volume ratio (20-100 vol%), NaOH concentration (5-15 wt%), and stirring rate (250-500 rpm) were investigated, and under optimum condition (60 vol% ethanol, 5 wt% NaOH, 80 °C), 95 % PET conversion was obtained [23].

The conventional alkaline hydrolysis occurs at a high temperature for a long duration, thus increasing the capital and operating cost of the overall process. Therefore, a novel and energy efficient economic and viable approach was employed for PET depolymerization under mild reaction conditions. In the present work, waste PET flakes depolymerization was studied at a moderate temperature by alkaline hydrolysis with *n*-propanol as a co-solvent. The effect of NaOH concentration and n-propanol to water volume ratio on PET conversion and TPA yield were experimentally explored. The experimentally obtained data were fitted against the solid-state kinetic models to find the best model for PET depolymerization in the studied conditions. Finally, the findings of the present work were compared with the available literature results in terms of PET conversion, TPA yield, and energy economy coefficient.

Experimental

Materials

Waste PET bottles (transparent drinking water, Brand: Alpine) were collected from the BIT Mesra Campus. Bottles were washed with a detergent in hot water to remove impurities such as dirt particles and oil components. It was again washed with hot water and dried in a hot air oven at 60 °C for 24 hours. After drying, bottles were manually cut into 0.5-1 cm × 0.5-1 cm flakes and used in alkaline hydrolysis experiments. *n*-propanol (99 % purity, CAS: 71-23-8) and Sodium hydroxide pellets (97 % purity, CAS: 1310-73-2) were supplied by Central Drug House (P) Limited. Sulphuric acid (98 % purity, CAS: 7664-93-9) was supplied by Rankem, Avantor Performance Materials India Limited. Millipore water (conductivity < 1 µS/cm) was used wherever required. All the chemicals were used without any further purification.

Alkaline hydrolysis of PET

In a typical experiment, 2 gm of PET flakes and 20 mL of liquid (*n*-propanol + water) were added to a three-necked glass flask fitted with a thermometer, a magnetic stirrer, and a reflux condenser. The flask was immersed in a silicone oil bath. Sodium hydroxide was added to the flask when the reaction mixture reached the target temperature. The reaction was performed at a constant temperature for 15-60 min under atmospheric pressure. The reaction conditions studied in the present work are reported in Table 1. In each experiment, the temperature was kept constant at 70 °C. *n*-propanol volume % in the liquid mixture was varied as 20 %, 40 % and 60 %. The experiment used two different NaOH concentrations, 5 % and 15 % (NaOH wt/liquid volume). After the completion of the reaction, the flask was immersed in an ice-water vessel to stop the reaction instantly. An excess amount of water was added to the reaction mixture, and un-depolymerized PET was separated by filtration. The un-depolymerized PET was dried in a hot air oven for specific hours and weighed. The conversion of PET was calculated as follows:

J. Mex. Chem. Soc. 2025, 69(3)
Regular Issue

ISSN-e 2594-0317

$$\%\text{Conversion} = \frac{\text{Initial weight of PET} - \text{Weight of undepolymerized PET}}{\text{Initial weight of PET}} \times 100 \quad (1)$$

Table 1. Different experimental conditions of alkaline hydrolysis done in the present work (2 g PET, 20 mL liquid (water + *n*-propanol), 400 rpm).

Sl. no.	*n*-propanol (vol%)	Temp (°C)	Time (min)	NaOH (%w/v)
Exp. 1	20 %	70	15	5
Exp. 2	20 %	70	30	5
Exp. 3	20 %	70	45	5
Exp. 4	20 %	70	60	5
Exp. 5	40 %	70	15	5
Exp. 6	40 %	70	30	5
Exp. 7	40 %	70	45	5
Exp. 8	40 %	70	60	5
Exp. 9	60 %	70	15	5
Exp. 10	60 %	70	30	5
Exp. 11	60 %	70	45	5
Exp. 12	60 %	70	60	5
Exp. 13	20 %	70	15	15
Exp. 14	20 %	70	30	15
Exp. 15	20 %	70	45	15
Exp. 16	20 %	70	60	15
Exp. 17	40 %	70	15	15
Exp. 18	40 %	70	30	15
Exp. 19	40 %	70	45	15
Exp. 20	40 %	70	60	15
Exp. 21	60 %	70	15	15
Exp. 22	60 %	70	30	15
Exp. 23	60 %	70	45	15
Exp. 24	60 %	70	60	15

The excess water was added to the filtrate to dissolve all the salt (disodium terephthalate). The resulting liquid mixture was acidified with sulphuric acid (H_2SO_4) to a pH of ~ 2-3 and left overnight. Finally, the liquid mixture was filtered and washed with water. The solid TPA obtained after filtration was dried in a hot air oven at 100 °C for 12 hours and weighed. TPA yield was calculated as follows:

$$\%\text{Yield} = \frac{\text{moles of TPA formed}}{\text{initial moles of PET}} \times 100 = \frac{\text{mass of TPA formed}/\text{MW}_{\text{TPA}}}{\text{initial mass of PET}/\text{MW}_{\text{PET}}} \times 100 \qquad (2)$$

where MW_{TPA} is the molecular weight of TPA (166 g/gmol), and MW_{PET} is the molecular weight of the PET repeating unit (192 g/gmol). A schematic of the PET alkaline hydrolysis process and reaction pathway is shown in Figures 1 and 2, respectively.

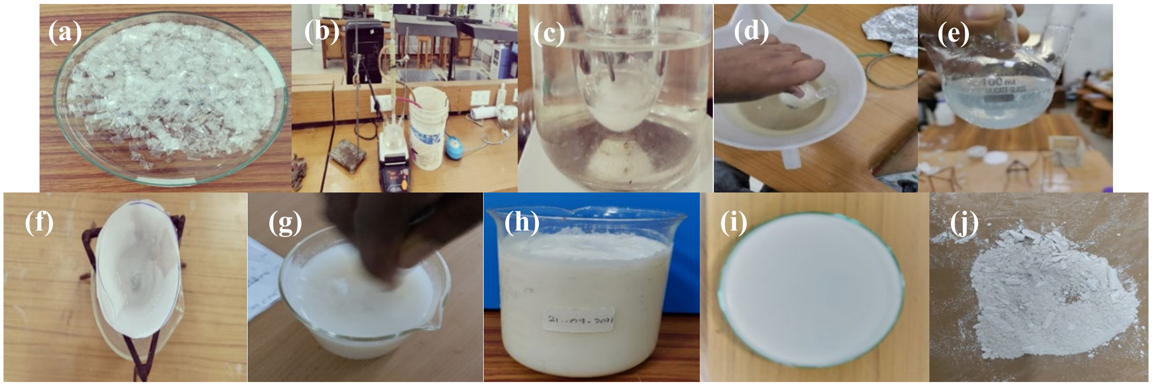

Fig. 1. Preparation of TPA from alkaline hydrolysis of waste PET flakes. **(a)** PET flakes, **(b)** Experimental Setup, **(c)** After 1 hr of reaction, **(d)** Reaction mixture cooling, **(e)** Water addition, **(f)** Filtration, **(g)** Titration with Sulphuric acid, **(h)** Addition of excess water, **(i)** TPA after filtration, **(j)** TPA after drying in the hot air oven.

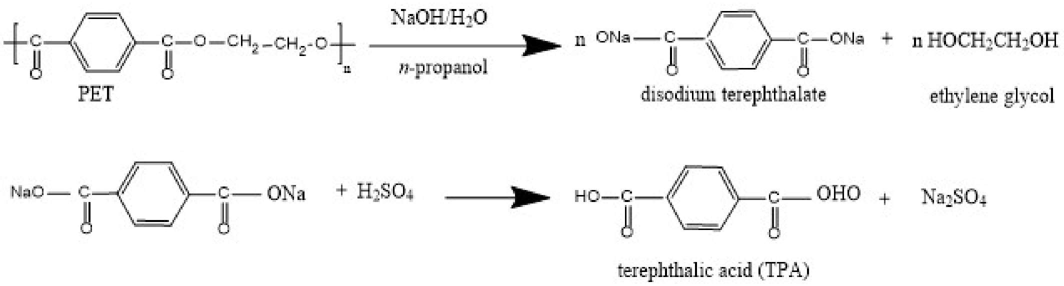

Fig. 2. Chemical Reaction for TPA Production through alkaline hydrolysis.

Characterization

Differential Scanning Calorimetry (DSC) measurements were done using Discovery DSC 25 (Waters, USA) under an N_2 atmosphere with a 20 mL/min flow. Each sample was heated starting from 40 °C to 300 °C and then cooled to 50 °C at a heating/cooling rate of 10 °C/min. The following equation was used to calculate the crystallinity of the PET sample:

J. Mex. Chem. Soc. 2025, 69(3)
Regular Issue

ISSN-e 2594-0317

$$X_C = \frac{\Delta H_m - \Delta H_{cc}}{\Delta H_m^{\circ}} \times 100 \tag{3}$$

where X_C is the crystallinity (%), ΔH_m (J/g) is the measured melt crystallization enthalpy of PET, ΔH_{cc} (J/g) is the measured cold crystallization enthalpy of PET and ΔH_m°=140.1 J/g is the melting enthalpy of 100 % crystalline PET. The DSC curve of waste PET flakes is shown in Fig. S1. Based on equation (3) and Fig. S1, the calculated crystallinity of waste PET flakes was 18 %.

Thermogravimetric analysis (TGA) (DTG-60, Shimadzu Corporation, Japan) was performed under an inert atmosphere (N_2 flow rate = 50 mL/min). About 3 mg of PET sample was placed in the crucible and heated from 28 °C to 750 °C with a heating rate of 10 °C/min. The TGA curve of waste PET flakes is shown in Fig. S2.

Fourier-transform infrared spectroscopy (FTIR) characterized both sides of PET flakes using Frontier, Perkin Elmer, USA, and shown in Fig. S3.

Results and discussion

Characterization of TPA

The synthesized TPA was analyzed using various analytical techniques such as p-XRD (Powder X-Ray Diffractometer, Smart Lab 9 KW, Rigaku, Japan), DSC, TGA, FTIR and NMR (Figures 3-7). p-XRD patterns for synthesized TPA exhibit characteristic peaks at 2θ values of 17.059°, 24.93°, and 27.72° (Fig. 3). These values match well with the reported values of synthesized as well as commercial TPA [24,25], confirming the formation of TPA by depolymerization of PET flakes. The DSC curve of the synthesized TPA is shown in Fig. 4, and there is a sharp endothermic peak at 392.67 °C which matches with the synthesized TPA (388 °C) and standard TPA (390 °C) as reported in the literature [26]. The TGA curve showed that thermal degradation of synthesized TPA started at 250 °C, and about 90 % mass loss was observed between 250-350 °C (Fig 5), which matches the reported data in the literature [27]. The FTIR spectrum was recorded in the wavelength range of (4000-500 cm^{-1}). Fig. 6 depicts the FTIR spectra of synthesized TPA, consistent with those reported in the literature [24]. The presence of a carboxylic group causes the typical bands to appear at 1280, 1676, and 2666 cm^{-1}, whereas an aromatic ring causes them to appear at 730 cm^{-1}. ^1H NMR (Nuclear Magnetic Resonance) analysis of the product was performed by a JEOL (JNM ECZ400S/LI, Japan) NMR spectrometer operating at 400 MHz in a dmso-d_6 solution. Fig. 7 shows the ^1H NMR analysis of TPA with two characteristic peaks, one at 8.0 ppm due to the presence of aromatic ring and another at 13 ppm due to the presence -OH group. ^1H NMR clearly shows the high purity of the synthesized TPA.

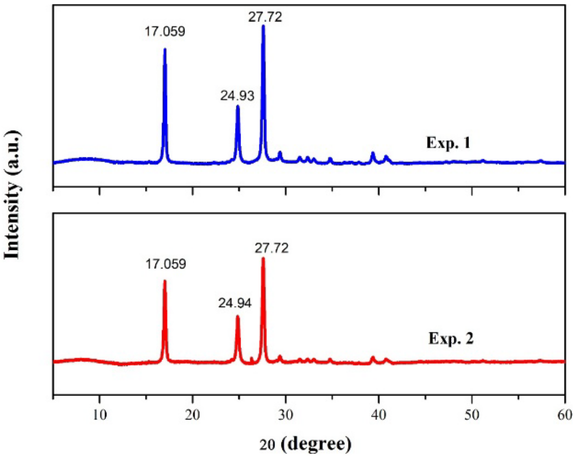

Fig. 3. p-XRD pattern of synthesized TPA.

J. Mex. Chem. Soc. **2025**, *69*(3)
Regular Issue

ISSN-e 2594-0317

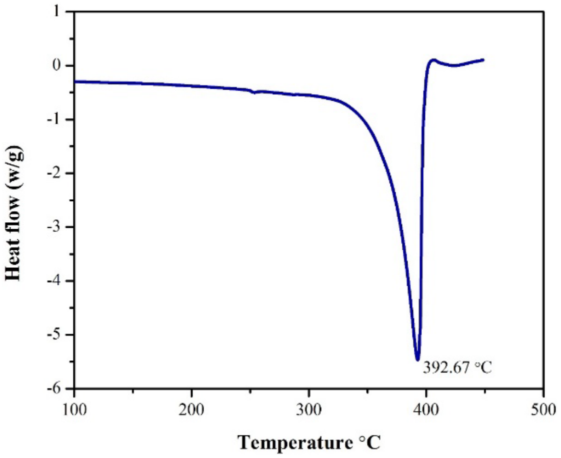

Fig. 4. DSC curve of synthesized TPA.

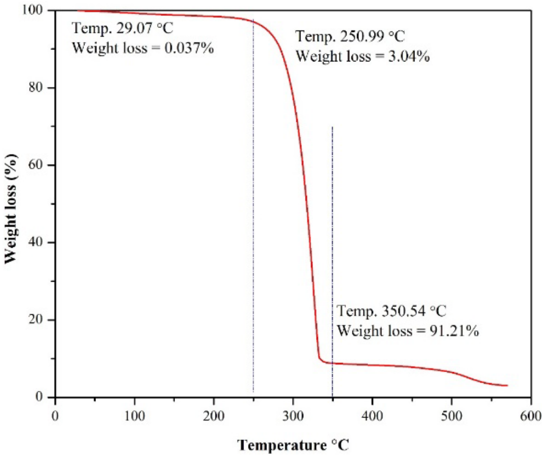

Fig. 5. TGA curve of synthesized TPA.

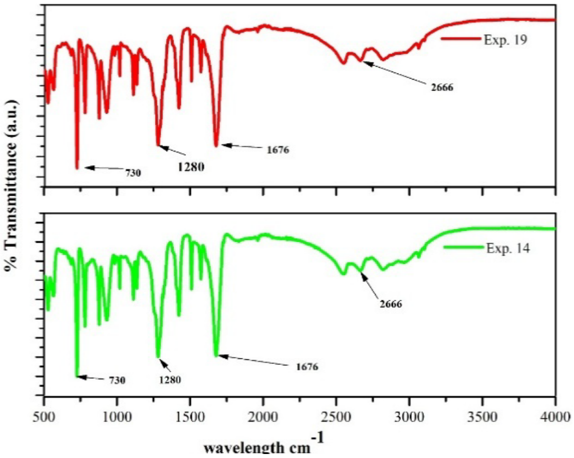

Fig. 6. FTIR spectra of synthesized TPA.

J. Mex. Chem. Soc. **2025**, *69*(3)
Regular Issue

ISSN-e 2594-0317

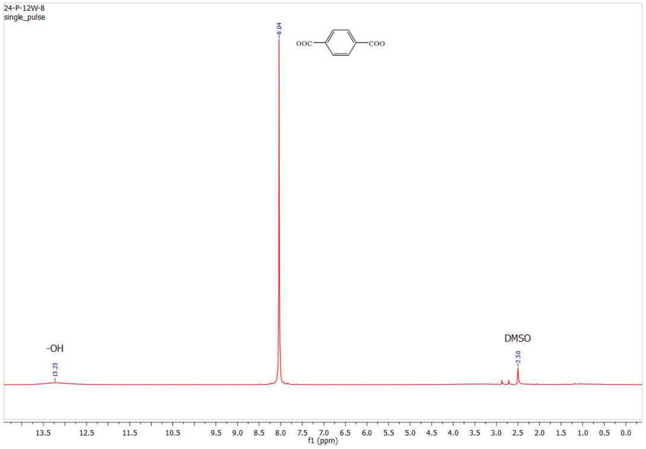

Fig. 7. ^{1}H NMR spectra of synthesized TPA.

Effect of reaction time

The effect of reaction time on PET conversion was investigated and presented in Fig. 8. PET conversion increased from 7.4 % to 21.8 % (20 vol% *n*-propanol), 15.1 % to 32.4 % (40 vol% *n*-propanol), and 27.8 % to 61.9 % (60 vol% *n*-propanol) as the reaction time increased from 15 min to 60 min with 5 wt/vol % of NaOH (Fig. 8**(a)**). The same behavior was observed with 15 wt/vol % NaOH concentration. PET conversion increased from 30 % to 73.5 % (20 vol% *n*-propanol), 49.1 % to 84.9 % (40 vol% *n*-propanol), and 52.8 % to 97.1 % (60 vol% *n*-propanol) as the reaction time increased from 15 min to 60 min (Fig. 8**(b)**). The effect of reaction time on TPA yield is shown in Fig. 9. At low concentrations of NaOH (5 wt/vol %), TPA yield increased from 2.0% to 11.2 %, 12.9 % to 29.3 %, and 17.0 % to 60.6 %, respectively for 20 vol%, 40 vol% and 60 vol% *n*-propanol. But at higher NaOH concentrations (15 wt/vol %) and higher *n*-propanol vol% (40 vol% and 60 vol%), TPA yield increased with increasing time, attained a maximum, and decreased. TPA yield increased from 49.3 % to 71.3 % as time increased from 15 min to 45 min and then reduced to 45.0 % as time increased from 45 min to 60 min (60 vol% *n*-propanol), as shown in Fig. 9**(b)**. It may be because higher NaOH concentration and *n*-propanol vol% increased catalytic activity, and thus maximum TPA yield was achieved in a shorter reaction time. Increasing reaction time led to side reactions, resulting in the formation of other products, and therefore the yield of TPA decreased.

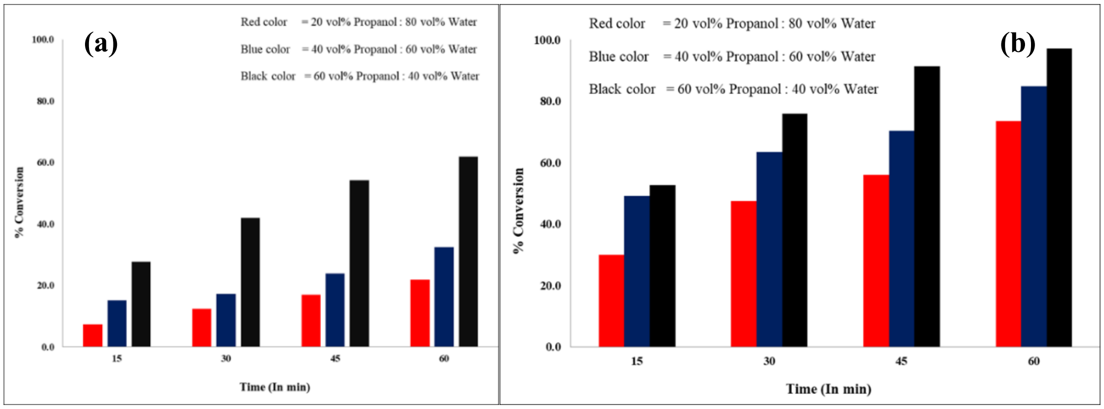

Fig. 8. PET Conversion at different experimental conditions (PET = 2 g, Alcohol + Water = 20 mL, Temp = 70 °C). **(a)** NaOH = 1 g, **(b)** NaOH = 3 g.

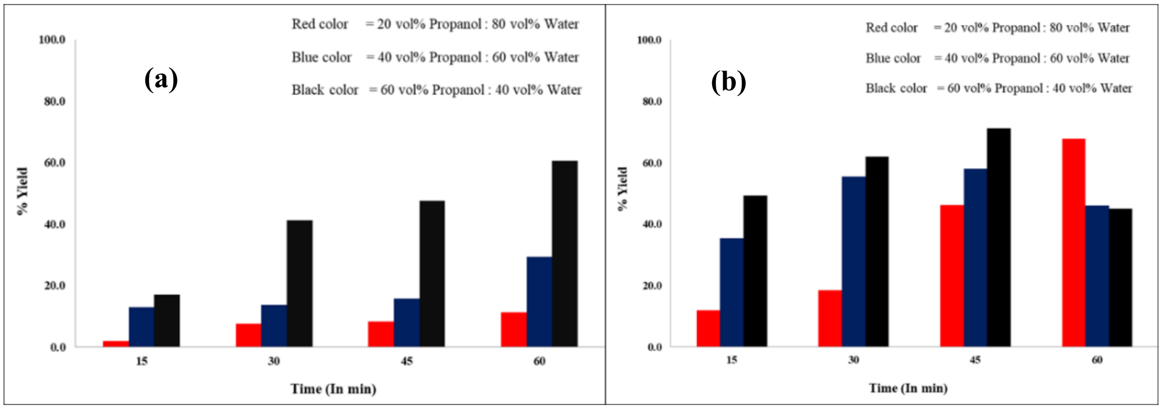

Fig. 9. TPA yield at different experimental conditions (PET = 2 g, Alcohol + Water = 20 mL, Temp = 70 °C). **(a)** NaOH = 1 g, **(b)** NaOH = 3 g.

Effect of co-solvent volume ratio

The impact of *n*-propanol as a co-solvent on PET conversion and TPA yield can be explained through Fig. 9. Increasing the vol% of *n*-propanol from 20 vol% to 60 vol% increased PET conversion significantly. PET conversion increased from 21.8 % to 61.9 % (5 wt/vol % NaOH) & 73.5 % to 97.1 % (15 wt/vol % NaOH) by increasing *n*-propanol vol% from 20 % to 60 % at a reaction time of 60 min. Ugduler et al. [23] observed a similar behavior while studying PET alkaline hydrolysis in the presence of ethanol as a co-solvent. The result of Ugduler et al. has been re-reported in Table 2. PET conversion increased from 68.32 % to 95.23 % (5 wt% NaOH), 70.47 % to 77.49 % (10 wt% NaOH), and 48.44 to 81.41 % (15 wt% NaOH) with an increase in ethanol vol% from 20 vol% to 60 vol%. The increase of vol% of *n*-propanol also impacted TPA yields. TPA yield increased from 11.2 % to 60.6 % for a reaction time of 60 min and 5 wt/vol % NaOH concentration. At higher concentrations of NaOH, for a reaction time of 15 min, 30 min, and 45 min, TPA yield increased with the increase in *n*-propanol vol% from 20 % to 60 %. But the TPA yield showed different behavior for a reaction time of 60 min. The prolonged reaction time and higher NaOH concentration reduced the effect of increased *n*-propanol vol% as TPA yield decreased from 67.8 % to 45.0 %.

Table 2. PET conversion (%) w.r.t. NaOH and EtOH concentration [Time = 20 min, Temp = 80 °C, PET = 2 g, EtOH + H_2O = 100 mL]

Sl. No.	NaOH (wt%)	EtOH (vol%)	PET conversion (%)
1	5	20	68.32
2	5	60	95.23
3	5	100	72.11
4	10	20	70.47
5	10	60	77.49
6	10	100	46.90
7	15	20	48.44
8	15	60	81.41

Effect of NaOH concentration

The effect of NaOH concentration on PET conversion and TPA yield is shown in Figures 10 and 11. PET conversion and TPA yield increased by increasing NaOH concentration from 5 wt/vol% to 15 wt/vol% for different reaction time conditions and ratios of *n*-propanol and water except in one situation. At 60 vol% *n*-propanol and a reaction time of 60 min, by increasing NaOH concentration from 5 wt/vol% to 15 wt/vol%, TPA yield decreased from 60.6 % to 45.0 %. As also reported by Ugduler et al. [23] with ethanol as a co-solvent, PET conversion increased slightly from 68.32 % (5 wt% NaOH) to 70.47 % (10 wt% NaOH) and then decreased to 48.44 % (15 wt% NaOH) at 20 vol% EtOH. But at 60 vol% EtOH, PET conversion decreased from 95.23 % (5 wt% NaOH) to 77.49 % (10 wt% NaOH) and then again slightly increased to 81.41 % (15 wt% NaOH) (Table 2). But in this work, NaOH concentration positively affects PET conversion with *n*-propanol as a co-solvent as opposed to work reported by Ugduler et al. [23] with ethanol as a co-solvent.

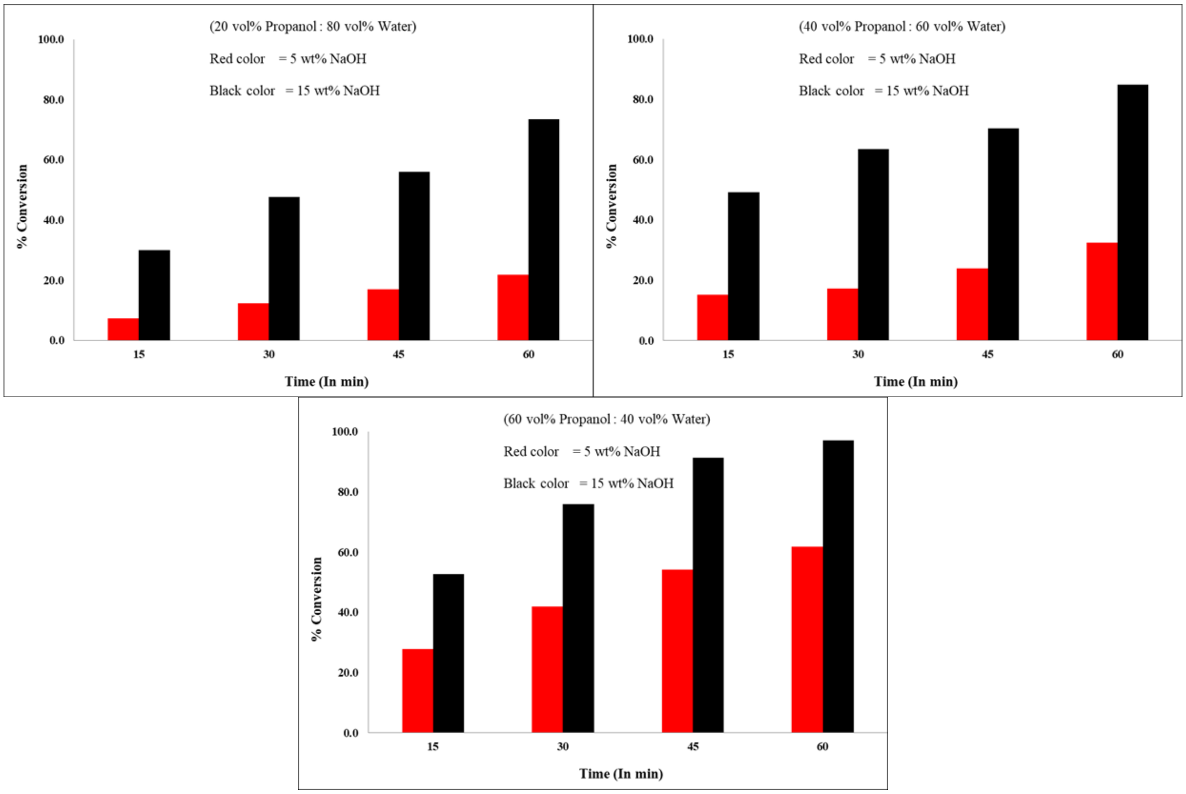

Fig.10. Effect of NaOH concentration on PET Conversion (PET = 2 g, Alcohol + Water = 20 ml, Temp = 70 °C).

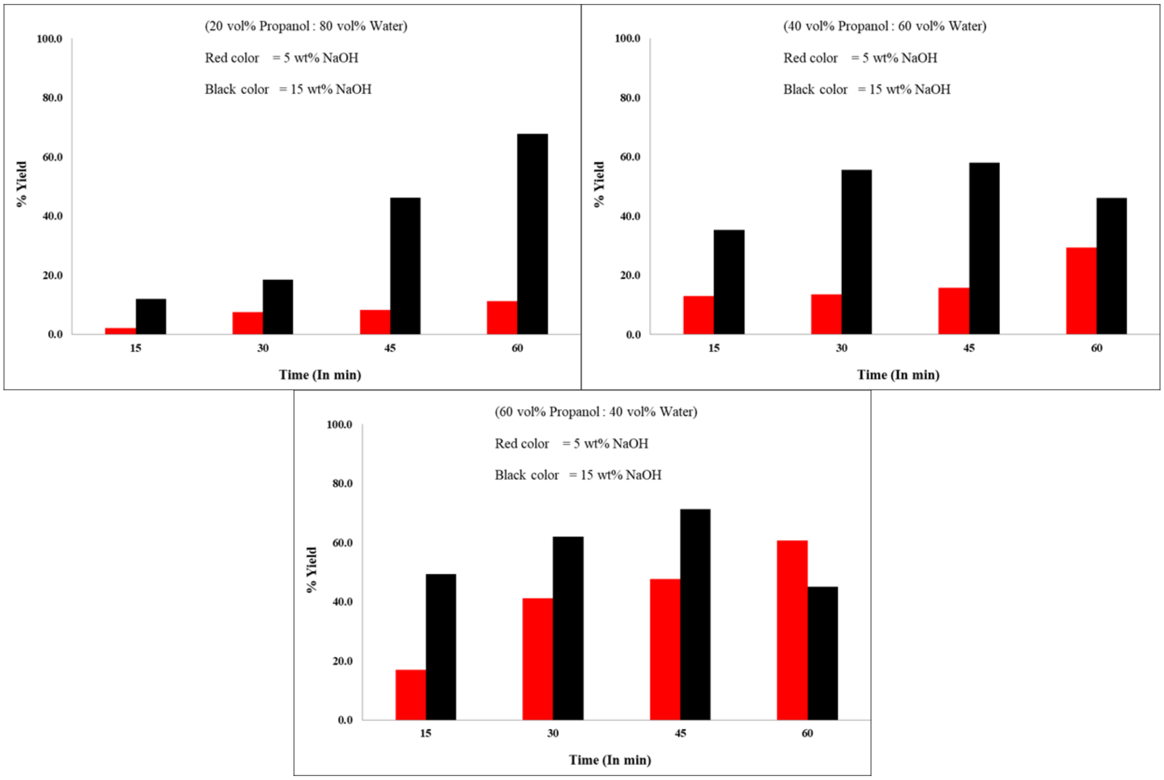

Fig. 11. Effect of NaOH concentration on TPA yield (PET = 2 g, Alcohol + Water = 20 mL, Temp = 70 °C).

Comparison with literature

Ugduler et al. [23] have reported the alkaline hydrolysis of different types of PET using ethanol as a co-solvent and NaOH as a catalyst. The experimental conditions reported by Ugduler et al. [23] with ethanol (Temp = 80 °C, Time = 20 min and solvent = 100 mL) as a co-solvent differ slightly from the present work on *n*-propanol (Temp = 70 °C, Time = 15 min and solvent = 20 mL) as a co-solvent. At low and high NaOH concentrations with different alcohol vol%, PET conversion with ethanol is much higher than *n*-propanol (Table 3). The PET conversion is 95.23 % with ethanol compared with 27.80 % with *n*-propanol at 60 vol% of alcohol at low NaOH concentrations. Similarly, PET conversion is 81.41 % with ethanol at high NaOH concentrations than 52.80 % with *n*-propanol. If we compare the results in terms of PET conversion, ethanol is better co-solvent compared to *n*-propanol for PET depolymerization. Barnard et al. [9] recently proposed an energy economy coefficient (ϵ) to compare different PET depolymerization processes. The energy economy coefficient is defined as:

$$\epsilon = \frac{\text{Yield (of the main monomer)}}{\text{Temperature (°C)} \times \text{Time (in minutes)}} \tag{4}$$

The ϵ-coefficient links the monomer yield to the temperature and time of the reaction. The lower the reaction time and temperature, the higher the ϵ-coefficient, and the better the process. Since, Ugduler et al. [11] have not reported the yield of monomer (TPA), the above equation has been modified to include PET conversion instead of monomer yield. Therefore, the modified energy economy coefficient is defined as:

$$\epsilon = \frac{\text{PET conversion}}{\text{Temperature (°C)} \times \text{Time (in minutes)}} \tag{5}$$

J. Mex. Chem. Soc. **2025**, *69*(3)
Regular Issue

ISSN-e 2594-0317

The higher the PET conversion and lower the reaction time and temperature, the higher the ϵ-coefficient, and the better the process. Table 4 shows that at lower NaOH concentrations, the energy economy coefficient is much higher for ethanol-based processes than for *n*-propanol-based processes. But at higher NaOH concentrations, ethanol, and *n*-propanol-based processes are comparable based on energy factor. It shows that PET depolymerization is not affected by carbon chain number of alcohol at higher NaOH concentrations.

Table 3. Comparison between EtOH and *n*-PrOH [Conditions for EtOH: Time = 20 min, Temp = 80 °C, PET = 2 g, EtOH + H_2O = 100 mL; Conditions for *n*-PrOH: Time = 15 min, Temp = 70 °C, PET = 2 g, *n*-PrOH + H_2O = 20 mL].

Sl. No.	NaOH (wt%)	EtOH (vol%)/ *n*-PrOH (vol%)	PET Conversion (%) (with EtOH)	PET Conversion (%) (with *n*-PrOH)	Energy Economy Co-efficient (ϵ) (with EtOH)	Energy Economy Co-efficient (ϵ) (with *n*-PrOH)
1	5	20	68.32	7.40	0.043	0.007
2	5	60	95.23	27.80	0.060	0.026
3	15	20	48.44	30.00	0.030	0.029
4	15	60	81.41	52.80	0.051	0.050

Table 4. Solid-state kinetic models.

Reaction Model	Integral form $g(\alpha) = kt$
Diffusion models	
1-D diffusion (D1)	α^2
2-D diffusion (D2)	$[(1-\alpha)\ln(1-\alpha)] + \alpha$
3-D diffusion-Jander (D3)	$[1-(1-\alpha)^{1/3}]^2$
Ginstling-Brounshtein (D4)	$1 - 2\alpha/3 - (1-\alpha)^{2/3}$
Geometrical contraction models	
Contracting area (R2)	$1-(1-\alpha)^{1/2}$
Contracting volume (R3)	$1-(1-\alpha)^{1/3}$
Reaction order models	
Zero-order (F0)	α
First-order (F1)	$-\ln(1-\alpha)$
Second-order (F2)	$(1-\alpha)^{-1} - 1$
Third-order (F3)	$(1/2)[(1-\alpha)^{-2} - 1]$

J. Mex. Chem. Soc. **2025**, 69(3)
Regular Issue

ISSN-e 2594-0317

Reaction Model	**Integral form $g(\alpha) = kt$**
Nucleation models	
Power law (P2)	$\alpha^{1/2}$
Power law (P3)	$\alpha^{1/3}$
Power law (P4)	$\alpha^{1/4}$
Avrami-Erofeyev (A2)	$[-\ln(1-\alpha)]^{1/2}$
Avrami-Erofeyev (A3)	$[-\ln(1-\alpha)]^{1/3}$
Avrami-Erofeyev (A4)	$[-\ln(1-\alpha)]^{1/4}$

PET depolymerization reaction kinetics

In the present work, PET depolymerization kinetics have been studied with the help of solid-state kinetic models, which have a theoretical physical meaning [28]. Based on certain mechanistic assumptions, many models have been developed in solid-state kinetics. Table 4 shows the different models based on mechanistic assumptions: diffusion, geometrical contraction, reaction order, and nucleation models. Sestak and Berggren have suggested a general mathematical form that represents all solid-state kinetic models [29]:

$$g(\alpha) = \alpha^m (1-\alpha)^n (-\ln(1-\alpha))^p \tag{6}$$

where m, n, and p are model-specific constants. The model variable' α' is the conversion fraction which is defined as:

$$\alpha = \frac{m_0 - m_t}{m_0 - m_\infty} \tag{7}$$

where m_O is the initial mass, m_t is the mass at any time t, and m_∞ is the residual mass. For PET depolymerization reaction, $m_\infty = 0$. Therefore, the conversion fraction is PET conversion which has been experimentally determined. From Table 5, experimental kinetic data obtained at different experimental conditions closely matches the diffusion and geometrical contraction models. Reaction order models F0 and F1 also predicted a close match with the experimental result. Reaction order model F1 gave the best fit to the experimental data with a linear correlation coefficient (R^2) of 0.9918. In reaction order models, the reaction mixture is assumed to be homogeneous. The reaction rate is proportional to the fraction remaining of reactant(s) raised to a particular power which is the reaction order and independent of the solvent concentration. It is believed that kinetic analysis methods force data into an order-based model that may not be appropriate. But in the present case, the first-order model matches closely with the experimental data at all conditions. The zero-order reaction also fits well with a linear correlation coefficient (R^2) of 0.9715. Geometrical contraction models R2 and R3 also gave excellent fit to the experimental data with linear correlation coefficients (R^2) of 0.9863 and 0.9897, respectively. These models assume that nucleation occurs rapidly on the surface of the crystal, and the progress of the resulting reaction interface toward the center of the crystal controls the degradation rate. In the contracting area (R2) model, the solid particle is assumed to have a cylindrical shape, whereas in the contracting volume (R3) model, the solid particle is considered to have spherical or cubical shapes. Among diffusion models, the one-dimensional (D1) diffusion model is the best followed by the two-dimensional model (D2), the three-dimensional model of Ginstling-Brounshtein (D4), and the three-dimensional diffusion model (D3). Unlike other models, nucleation models gave less satisfactory results with linear correlation coefficients (R^2) of less than 0.95. Among the nucleation models, the Avrami models were better than the power law models, with R^2 values in the range of 0.90 to 0.95. Based on the above discussions,

ISSN-e 2594-0317

it may be concluded that the first-order reaction, geometrical contraction, and one-dimensional diffusion models are the best-fit kinetic models for the alkaline hydrolysis of PET.

Table 5. R^2-values for different kinetic models.

Reaction Model	**R^2-value**
Diffusion models	
1-D diffusion (D1)	0.9838
2-D diffusion (D2)	0.9788
3-D diffusion-Jander (D3)	0.9616
Ginstling-Brounshtein (D4)	0.9746
Geometrical contraction models	
Contracting area (R2)	0.9863
Contracting volume (R3)	0.9897
Reaction order models	
Zero-order (F0)	0.9715
First-order (F1)	0.9918
Second-order (F2)	0.9457
Third-order (F3)	0.8740
Nucleation models	
Power law (P2)	0.9218
Power law (P3)	0.8967
Power law (P4)	0.8824
Avrami-Erofeyev (A2)	0.9532
Avrami-Erofeyev (A3)	0.9227
Avrami-Erofeyev (A4)	0.9039

Conclusions

In the current study, the hydrolysis of waste PET was investigated using *n*-propanol as a co-solvent and NaOH as a catalyst at mild operating conditions. The effects of reaction time, *n*-propanol vol%, and NaOH concentration on PET conversion and TPA yield were investigated. All three parameters greatly affected PET

ISSN-e 2594-0317

depolymerization. It was found that the PET conversion and TPA yield reached 91.4 % and 71.3 %, respectively, under the conditions of 60 vol% *n*-propanol, 15 wt% NaOH, and at 70 °C in 45 minutes. The different characterization showed that the synthesized monomer was TPA of high purity. The best solid-state kinetic models were a first-order reaction, geometrical contraction, and one-dimensional diffusion models. The energy economy coefficient, which measures the energy efficiency of the process, was used to compare the performance of *n*-propanol as a co-solvent with other co-solvents reported in the literature. It was found that *n*-propanol as a co-solvent is as efficient as ethanol at high NaOH concentration (15 wt/vol%). This work showed that two-step alkaline hydrolysis of waste PET with NaOH as a catalyst and *n*-propanol as a co-solvent is an energy-efficient process with mild operating conditions and shorter reaction time. Finally, the present work showed that waste PET might be depolymerized into useful monomers with readily available materials in easy steps.

Acknowledgments

The authors thankfully acknowledge the Department of Chemical Engineering, BIT Mesra, Ranchi, for providing the necessary facilities for this research. The authors also acknowledge Central Instruments Facility, BIT Mesra, Ranchi, for performing DSC, TGA, FTIR, NMR and p-XRD characterization.

References

1. Global Plastics Outlook, OECD, **2022**. DOI: https://doi.org/10.1787/de747aef-en.
2. de Dios Caputto, M.D.; Navarro, R.; Valentín, J. López; Marcos-Fernandez, A. *J. Clean. Prod.* **2024**, *454*, 142253. DOI: https://doi.org/10.1016/j.jclepro.2024.142253.
3. Geyer, R.; Jambeck, J.R.; Law, K.L. *Sci. Adv.* **2017**, *3*, e1700782. DOI: https://doi.org/10.1126/sciadv.1700782.
4. Joseph, T. M.; Azat, S.; Ahmadi, Z.; Jazani, O. M.; Esmaeili, A.; Kianfar, E.; Haponiuk, J.; Thomas, S. *Case Stud. Chem. Environ. Eng.* **2024**, *9*, 100673. DOI: https://doi.org/10.1016/j.cscee.2024.100673.
5. Jambeck, J.R.; Geyer, R.; Wilcox, C.; Siegler, T.R.; Perryman, M.; Andrady, A.; Narayan, R.; Law, K.L. *Science.* **2015**, *347*, 768–771. DOI: https://doi.org/10.1126/science.1260352.
6. Shojaei, B.; Abtahi, M.; Najafi, M. *Polym. Adv. Technol.* **2020**, *31*, 2912–2938. DOI: https://doi.org/10.1002/pat.5023.
7. Rahimi, A.; García, J.M. *Nat. Rev. Chem.* **2017**, *1*, 0046. DOI: https://doi.org/10.1038/s41570-017-0046.
8. Sinha, V.; Patel, M.R.; Patel, J.V. *J. Polym. Environ.* **2010**, *18*, 8–25. DOI: https://doi.org/10.1007/s10924-008-0106-7.
9. Thiounn, T.; Smith, R.C. *J. Polym. Sci.* **2020**, *58*, 1347–1364. DOI: https://doi.org/10.1002/pol.20190261.
10. Raheem, A.B.; Noor, Z.Z.; Hassan, A.; Abd Hamid, M.K.; Samsudin, S.A.; Sabeen, A.H. *J. Clean. Prod.* **2019**, *225*, 1052–1064. DOI: https://doi.org/10.1016/j.jclepro.2019.04.019.
11. Barnard, E.; Rubio Arias, J.J.; Thielemans, W. *Green Chem.* **2021**, *23*, 3765–3789. DOI: https://doi.org/10.1039/D1GC00887K.
12. Chen, H.; Wan, K.; Zhang, Y.; Wang, Y. *ChemSusChem.* **2021**, *14*, 4123–4136. DOI: https://doi.org/10.1002/cssc.202100652.
13. Zhao, Y.B.; Lv, X.D.; Ni, H.G. *Chemosphere.* **2018**, *209*, 707–720. DOI: https://doi.org/10.1016/j.chemosphere.2018.06.095.

J. Mex. Chem. Soc. **2025**, *69*(3)
Regular Issue

ISSN-e 2594-0317

14. Vollmer, I.; Jenks, M.J.F.; Roelands, M.C.P.; White, R.J.; Harmelen, T.; Wild, P.; Laan, G.P.; Meirer, F.; Keurentjes, J.T.F.; Weckhuysen, B.M. *Angew. Chem. Int. Ed.* **2020**, *59*, 15402–15423. DOI: https://doi.org/10.1002/anie.201915651.
15. Jehanno, C.; Alty, J.W.; Roosen, M.; De Meester, S.; Dove, A.P.; Chen, E.Y.X.; Leibfarth, F.A.; Sardon, H. *Nature.* **2022**, *603*, 803–814. DOI: https://doi.org/10.1038/s41586-021-04350-0.
16. Olazabal, I.; Luna Barrios, E.J.; De Meester, S.; Jehanno, C.; Sardon, H. *ACS Appl. Polym. Mater.* **2024**, *6*, 4226–4232. DOI: https://doi.org/10.1021/acsapm.4c00326.
17. Hu, L.C.; Oku, A.; Yamada, E.; Tomari, K. *Polym. J.* **1997**, *29*, 708–712. DOI: https://doi.org/10.1295/polymj.29.708.
18. Kosmidis, V.A.; Achilias, D.S.; Karayannidis, G.P. *Macromol. Mater. Eng.* **2001**, *286*, 640–647. DOI: https://doi.org/10.1002/1439-2054(20011001)286:10<640::AID-MAME640>3.0.CO;2-1.
19. Karayannidis, G.P.; Chatziavgoustis, A.P.; Achilias, D.S. *Adv. Polym. Technol.* **2002**, *21*, 250–259. DOI: https://doi.org/10.1002/adv.10029.
20. Mishra, S.; Zope, V.; Goje, A. *Polym. Int.* **2002**, *51*, 1310–1315. DOI: https://doi.org/10.1002/pi.873.
21. Mishra, S.; Goje, A.S. *Polym. React. Eng.* **2003**, *11*, 963–987. DOI: https://doi.org/10.1081/PRE-120026382.
22. Khalaf, H.I.; Hasan, O.A. *Chem. Eng. J.* **2012**, *192*, 45–48. DOI: https://doi.org/10.1016/j.cej.2012.03.081.
23. Ügdüler, S.; Van Geem, K.M.; Denolf, R.; Roosen, M.; Mys, N.; Ragaert, K.; De Meester, S. *Green Chem.* **2020**, *22*, 5376–5394. DOI: https://doi.org/10.1039/D0GC00894J.
24. Panda, D.; Patra, S.; Awasthi, M.K.; Singh, S.K. *J. Chem. Educ.* **2020**, *97*, 1101–1108. DOI: https://doi.org/10.1021/acs.jchemed.9b00337.
25. Cosimbescu, L.; Merkel, D.R.; Darsell, J.; Petrossian, G. *Ind. Eng. Chem. Res.* **2021**, *60*, 12792–12797. DOI: https://doi.org/10.1021/acs.iecr.1c02604.
26. Parab, Y.S.; Shukla, S.R. *J. Macromol. Sci. Part A.* **2013**, *50*, 1149–1156. DOI: https://doi.org/10.1080/10601325.2013.830004.
27. Ravichandran, S.A.; Rajan, V.P.; Aravind, P.V.; Seenivasan, A.; Prakash, D.G.; Ramakrishnan, K. *Macromol. Symp.* **2016**, *361*, 30–33. DOI: https://doi.org/10.1002/masy.201400269.
28. Khawam, A.; Flanagan, D.R. *J. Phys. Chem. B.* **2006**, *110*, 17315–17328. DOI: https://doi.org/10.1021/jp062746a.
29. Šesták, J.; Berggren, G. *Thermochim. Acta.* **1971**, *3*, 1–12. DOI: https://doi.org/10.1016/0040-6031(71)85051-7.